# ANALIZA TERMICĂ A STICLELOR BIOACTIVE MEZOPOROASE ŞI MACROPOROASE SINTETIZATE PRIN METODA SOL-GEL

# THERMAL ANALYSIS OF MESOPOROUS AND MACROPOROUS BIOACTIVE GLASSES SYNTHESIZED BY SOL-GEL METHOD

**THANIDA CHAROENSUK**, **CHITNARONG SIRISATHITKUL**[*], **UPSORN BOONYANG**
*Molecular Technology Research Unit, School of Science, Walailak University, Nakhon Si Thammarat, 80161, Thailand*

***Sol-gel derived porous bioactive glasses were prepared by using the dual-templating method. Block copolymers used as one template component produced mesopores and the polymethyl methacrylate (PMMA) colloidal crystals as the other template component yielded three-dimensionally ordered macroporous bioactive glasses (3DOM-BG). The dual-templating 3DOM-BG with two different compositions exhibited greater weight loss in thermogravimetric analysis (TGA) and larger heat release in the major exothermic peak in differential thermal analysis (DTA) than the single-templating counterparts. It can be concluded that 3DOM-BG have higher crystalline phase and moisture absorption in their scaffolds.***

***Au fost preparate sticle bioactive poroase prin sol-gel folosind metoda cu şablon dublu. Copolimerii bloc utilizaţi ca un component al şablonului au produs mezopori iar cristalele coloidale de polimetacrilat de metil (PMMA) ca a doua componentă a şablonului au condus la sticle bioactive macroporoase tridimensional ordonate (3DOM-BG). Şablonul dublu 3DOM-BG cu două compoziţii diferite prezintă o pierdere în greutate mai mare la analiza termogravimetrică (TGA) şi o eliberare de căldură mai mare în vârful exotermic principal la analiza termică diferenţială (DTA) decât etapele singulare ale şablonului. Se poate concluziona că 3DOM-BG prezintă o fază cristalină şi o absorbţie de umiditate mai mare în eşafodajul lor.***

***Keywords:*** *Porous bioactive glass, sol-gel, crystallization, thermal properties*

## 1. Introduction

Mesoporous bioactive glasses (MBG) have recently attracted significant interests in bone tissue engineering. The bioactivity and biodegradable in the regeneration of bone defects are increased compared to traditional bioactive glasses owing to the large surface area and volume in their porous structures [1-3]. The sol-gel method becomes an attractive route to derive biomaterials with various advantages over the melt-derived products [4]. Sol-gel glasses can be prepared at low temperatures using hydrolysis and polycondensation process of alkoxides with the addition of bioactive modifiers. High surface area and volume of porosity are obtained from this process in a wide range of bioactive compositions (up to 90 % mol $SiO_2$) [1,5]. To produce mesoporous structures (2-50 nm in diameter), nontoxic difunctional non-ionic block copolymer surfactants such as P123, F127, and CTAB have been used [2]. To support the bone growth, macroporous structures (> 50 nm in diameter) were fabricated by using the porogens such as polymethyl methacrylate (PMMA), polyurethane sponge and foaming agents (e.g., polyethylene glycols, polyurethane foams and polylactide foams) as templates [6-7]. This porosity provides the scaffolds which areas for developing the vascular system and tailoring the new bone. Furthermore, their structures are also beneficial for bioresorption, biodegradation and bioactivity properties [8-10].

In this work, the PMMA colloidal crystal is selected as the template of macroporous frameworks for the sol-gel derived three-dimensional macroporous bioactive glass scaffolds (3DOM-BG). PMMA templates were prepared by a published method [11]. Upon the heat treatment, the PMMA template can easily be removed without fracturing of the three-dimensional network of glass [6]. Differences between thermal properties of 3DOM-BG and MBG are investigated by thermogravimetric analysis (TGA), derivative thermogravimetry (DTG) and differential thermal analysis (DTA).

## 2. Experimental

The single-templating MBG and dual-templating 3DOM-BG were prepared by using the sol-gel method. In the presence of surfactant and acid catalysts, tetraethyl orthosilicate (TEOS) was slowly mixed with bioactive modifiers including calcium nitrate tetrahydrate ($Ca(NO_3)_2{\cdot}4H_2O$), sodium nitrate ($NaNO_3$) and triethyl phosphate

[*] Autor corespondent/*Corresponding author*,
Tel.: +6675 672945, e-mail: chitnarong.siri@gmail.com

(TEP). The mixture was turbulently stirred to obtain a clear solution at room temperature. The solution was then aged at 60 °C in a vial allowing the hydrolysis and polycondensation processes before turning into the gel. In this aging step, two different conditions were applied by normal aging for MBG and by immersion of PMMA templates in the solution before aging for 3DOM-BG. The products were dried at the same temperature to allow the evaporation of excess solvents, catalysts, and by-products for one day. Finally, the calcination of dried gels at 600 °C for 6 hours activated the thermal decomposition of templates yielding the MBG and 3DOM-BG. To investigate the variation of thermal properties on the composition, two more samples with and without PMMA templates were synthesized by increasing the molar ratio of Si to Ca in the absence of Na as summarized in Table 1.

Morphology of the samples was characterized by scanning electron microscopy (SEM) (JEOL JSM-5410) and their compositions were analyzed by energy dispersive spectrometry (EDS) (INCA 300, Oxford). To study thermal properties of MBG and 3DOM-BG after the template removal, the thermogravimetric analysis (TGA) with its derivative thermogravimetry (DTG) and the differential thermal analysis (DTA) with the heating rate 10 °C/min from 50 °C up to 1,300 °C under $N_2$ atmosphere were carried out on the samples in thermal analysis system (Perkin-Elmer, 7 series). The TGA measures the mass change of the bioactive glasses as a function of temperature whereas the DTA measures the temperature difference of the sample versus a reference, caused by thermal properties of the sample.

## 3. Results and Discussion

In the initial stages of the sol-gel synthesis described in Eqs. (1)-(3), silanol [≡Si–OH] is formed by hydrolysis reactions of silicon alkoxides [TEOS; $Si(OCH_2CH_3)_4$; $Si(OR)_4$] and the condensation reactions then results in the siloxane [≡Si–O–Si≡] [12-17].

Hydrolysis : $Si(OR)_4 + nH_2O \rightarrow Si(OR)_{(4-n)}(OH)_n + nROH$ (1)

Water condensation : $\equiv Si{-}OH + HO{-}Si\equiv \rightarrow \equiv Si{-}O{-}Si\equiv + H_2O$ (2)

Alcohol condensation : $\equiv Si{-}OH + RO{-}Si\equiv \rightarrow \equiv Si{-}O{-}Si\equiv + ROH$ (3)

The hydrolysis reaction can be accelerated by the addition of acid catalyst due to the protonation of alkoxide [14].

$H_2O + Si(OR)_3(OHR)^+ \rightarrow (H_2O)^{\delta+}\ldots Si(OR)_3\ldots(OHR)^{\delta+}$ (4)

$(H_2O)^{\delta+}\ldots Si(OR)_3\ldots(OHR)^{\delta+} \rightarrow Si(OR)_3OH + ROH + H^+$ (5)

The gel is formed in the polycondensation reaction with the siloxane monomers turning into oligomers. The aggregation and the growing clusters of the polymerization network results in the gelation mechanisms. $Ca^{2+}$ and $Na^+$ ions are incorporated into the gel by attracting to nonbridging oxygen atoms [18].

$Ca^{2+} + 2[\equiv Si{-}OH] \rightarrow \equiv Si{-}O\ldots Ca\ldots O{-}Si\equiv + 2H^+$ (6)

$Na^+ + \equiv Si{-}OH \rightarrow \equiv Si{-}O\ldots Na + H^+$ (7)

The EDS spectra in Figure 1 confirm the phases of sol-gel derived 59S MBG and

**Table 1**

Sol-gel synthesis conditions for MBG and 3DOM-BG/ *Condiţiile de sinteză sol-gel pentru MBG şi 3DOM-BG*

| Samples ID *Identificator probă* | template şablon | Molar ratio *Fracţie molară* Si/Ca/Na/P | Chemicals and reagents / *Reactivi chimici* | | | | | | |
|---|---|---|---|---|---|---|---|---|---|
| | | | TEOS (ml) | $Ca(NO_3)_2 \cdot 4H_2O$ (g) | 1M $NaNO_3$ (ml) | TEP (ml) | Surfactant | Catalyst *Catalizator* | solvent |
| 59S MBG | - | 59/35/2/4 | 1.29 | 0.81 | 0.40 | 0.12 | 0.49 g F127 | 1 ml (1M)$HNO_3$ 0.50 ml $C_6H_8O_7$ | - |
| 59S 3DOM-BG | PMMA | | | | | | | | |
| 80S MBG | - | 80/15/0/5 | 1.67 | 0.35 | - | 0.18 | 1.00 g P123 | 0.25 ml (0.5M)HCl | 2 ml ethanol |
| 80S 3DOM-BG | PMMA | | | | | | | | |

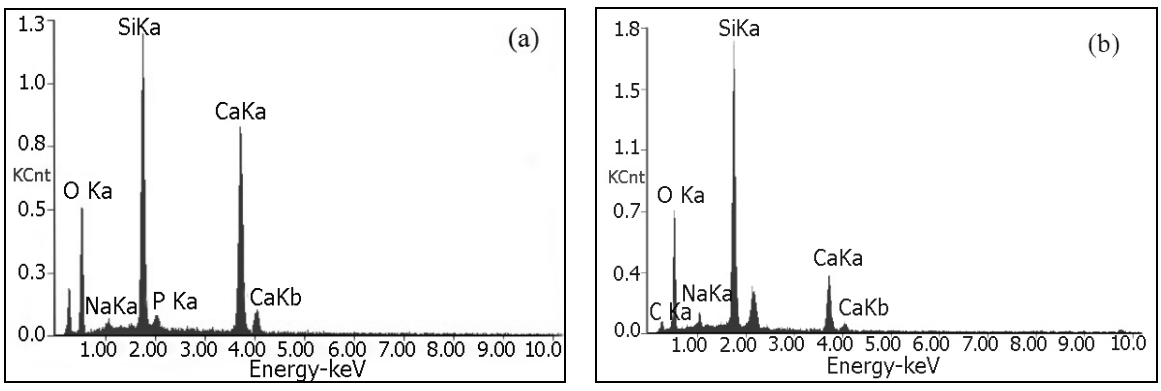


Fig. 1 - EDS spectra of (a) 59S MBG and (b) 59S 3DOM-BG./ *Spectrele EDS ale (a) 59S MBG şi (b) 59S 3DOM-BG.*

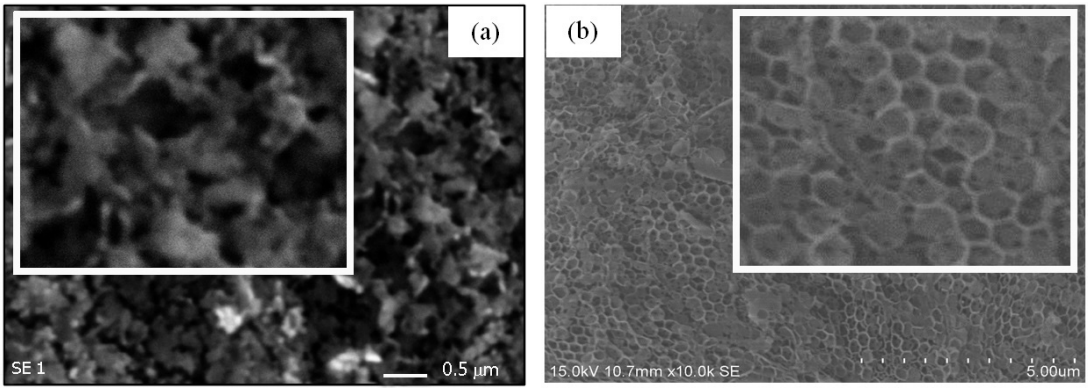


Fig. 2 - SEM images of samples (a) 59S MBG and (b) 59S 3DOM-BG. Insets show higher magnifications. /*Micrografii SEM ale probelor (a) 59S MBG şi (b) 59S 3DOM-BG. Medalioanele prezintă măriri mai mari.*

59S 3DOM-BG. Bioactivity substances such as Ca, Na, and P which are the elemental compositions of bioactive glass are detected in both samples. Interestingly, the ratio of Ca to Na peak intensity is significantly higher in the case of 59S MBG. Moreover, these EDS spectra indicate the purity of glasses by showing no impurity peak.

Figure 2 compares the morphology of samples 59S MBG and 59S 3DOM-BG. Figure 2(a) reveals an irregular porous structure with a large variation of mesopores and macropores in the 59S MBG. By contrast, the 59S 3DOM-BG in Figure 2(b) exhibits a three dimensional porous scaffolds with two different pore sizes. The regularity of the mesopores distributed inside the macropores occurs after the elimination of the spherical PMMA templates [6,8,15,19].

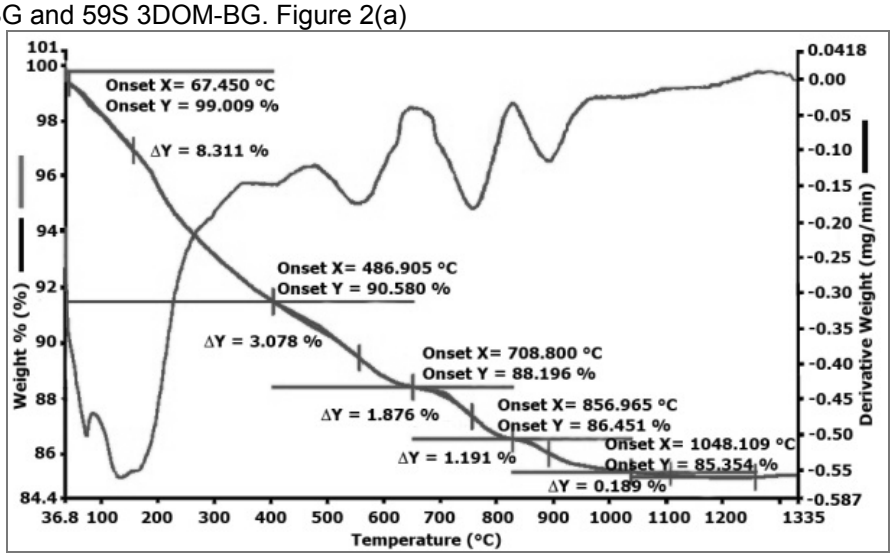


a

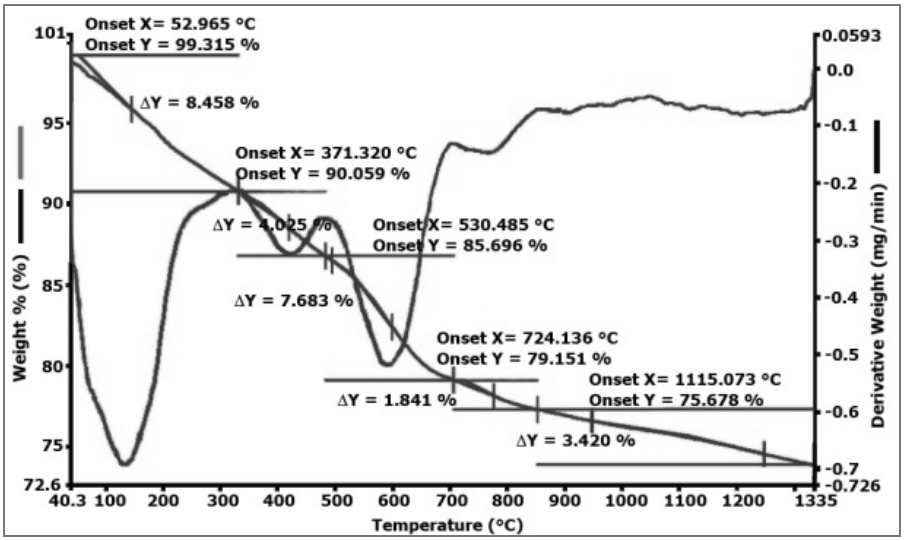


b

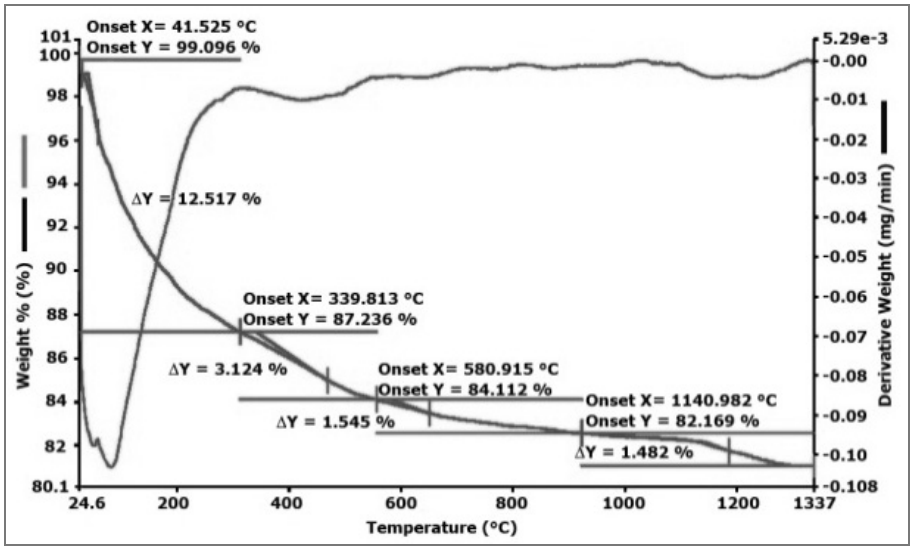


c

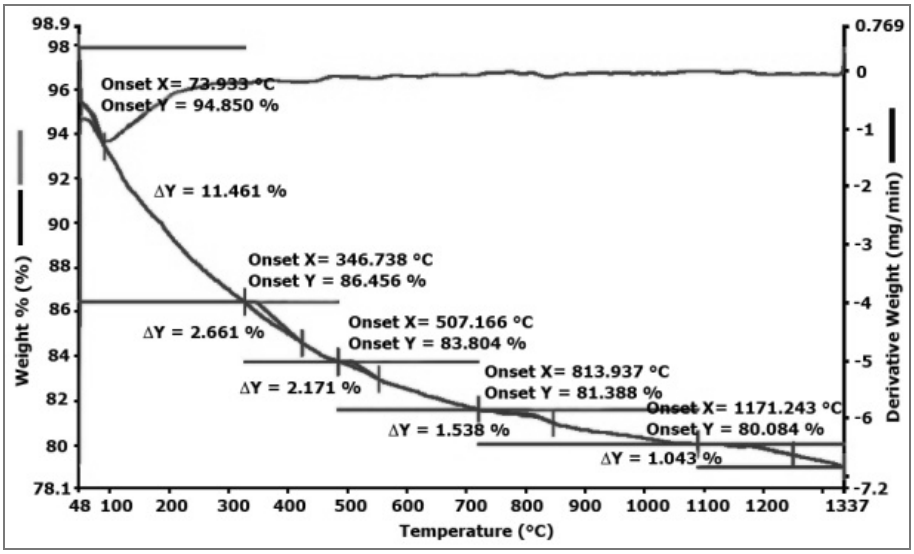


d

Fig. 3 - TGA/DTG curves of samples (a) 59S MBG, (b) 59S 3DOM-BG, (c) 80S MBG and (d) 80S 3DOM-BG. / *Curbele TGA/DTG pentru probele (a) 59S MBG, (b) 59S 3DOM-BG, (c) 80S MBG şi (d) 80S 3DOM-BG.*

Figure 3(a)-(b) shows the curves from TGA plotted with DTG of samples 59S MBG and 59S 3DOM-BG, respectively. Overall, 59S 3DOM-BG exhibits a greater weight loss. The first weight losses of approximately 8% from the removal of adsorbed water physically trapped in the pores [20-23] are observed in both TGA curves but the onset for the 59S MBG at 67 °C is higher than 53 °C in the 59S 3DOM-BG. The corresponding DTG curve of the 59S MBG also has a large dip at a higher temperature. These observations are related to DTA curves shown in Figure 4(a)-(b). The endothermic peak around 95 °C with a much larger area indicates a larger heat consumption in residual dehydration in the case of 59S 3DOM-BG. As the temperature increased to the second and third weight losses, 59S 3DOM-BG still exhibits lower onset temperatures with higher losses. In stabilized samples, such losses are due to structural densification whereas the thermal decomposition of residual precursors is absent and not evident in DTA curves [18]. The fourth weight loss of less than 2 % above 700 °C in DTG curves is due to the crystallization in glassy matrix [23-25]. These features in TGA/DTG curves are related to the broad exothermic peak around 810 °C in DTA curves. The area beneath this peak corresponding to the amount of heat release in the process is much larger for 59S 3DOM-BG. This implies the enhancement of crystallization in the 59S 3DOM-BG. Furthermore, 59S MBG has another exothermic peak at a slightly higher temperature which possibly reflecting the irregularity of its structure. Finally, the weight losses observed in TGA curves above 1000 °C are due to the melting whose onset temperature is higher in the case of 59S 3DOM-BG.

With a variation in the composition, some trends are similarly observed in Figures 3(c)-(d) and 4(c)-(d). The area beneath the major exothermic DTA peak of 80S 3DOM-BG is larger

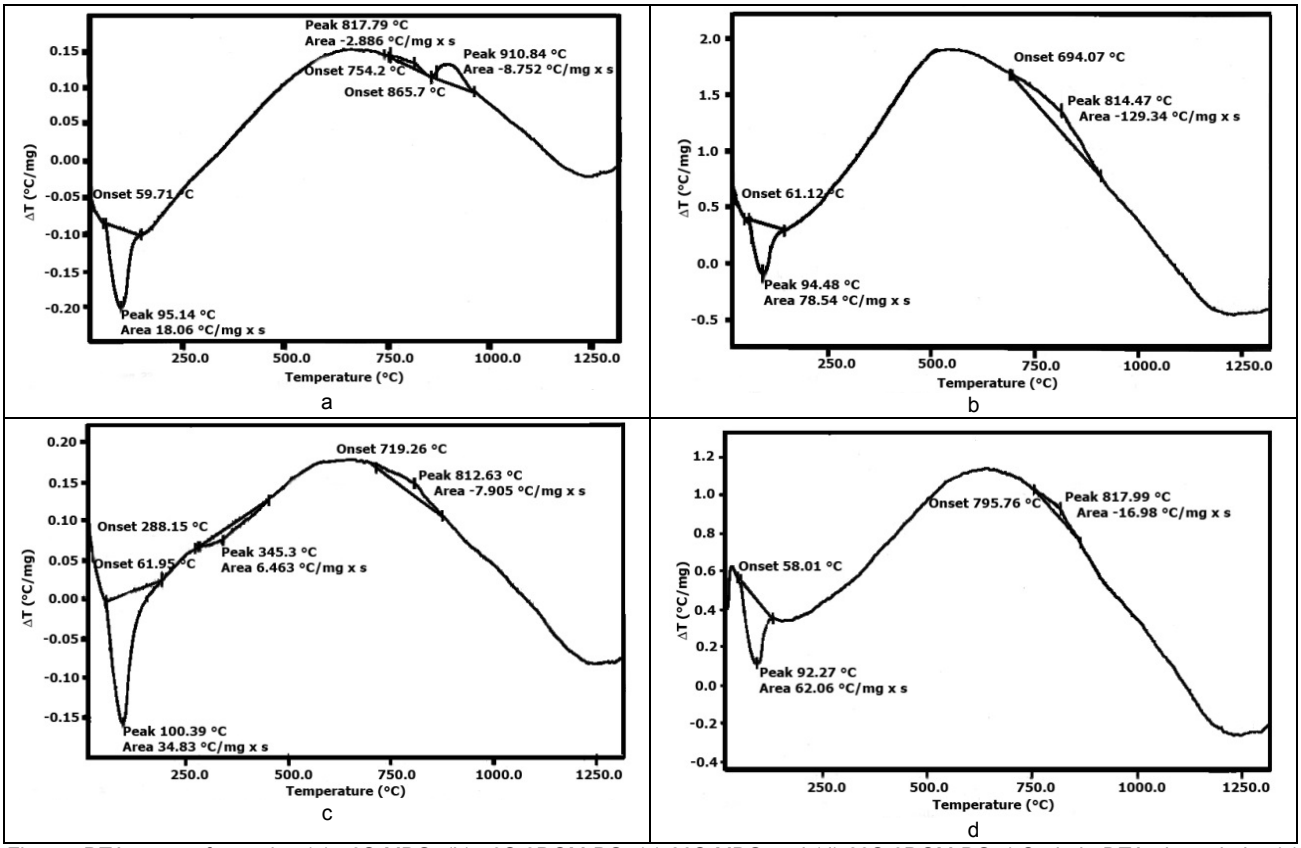


Fig. 4 - DTA curve of samples (a) 59S MBG, (b) 59S 3DOM-BG, (c) 80S MBG and (d) 80S 3DOM-BG. / *Curbele DTA ale probelor (a) 59S MBG, (b) 59S 3DOM-BG, (c) 80S MBG şi (d) 80S 3DOM-BG.*

than that of 80S MBG. This result underlines the dependence of crystallization of porous bioactive glasses on the PMMA templates during the synthesis. The total weight loss of sample 80S 3DOM-BG measured by TGA is also greater with more heat in the major endothermic transition due to the moisture reduction. These occurrences in both compositions are explained by larger amount of absorbed water in three dimensional porous scaffolds. Finally, the onset of weight loss due to the melting of 80S 3DOM-BG is higher than that of 80S MBG. Without Na, 80S samples have higher melting points and lower crystalline phases compared to those of 59S counterparts [3].

## 4. Conclusions

1. 3DOM-BG with mesopores in ordered macropores can be obtained by using PMMA templates in the sol-gel synthesis.

2. Compared to TGA of MBG from identical precursors, 3DOM-BG show greater first weight loss indicating more adsorbed water trapped in the scaffolds and higher onset temperature of the final weight loss from melting.

3. Compared to DTA of MBG from identical precursors, 3DOM-BG show larger heat release in the major exothermic peak indicating the increase in crystalline phase.

4. The inclusion of Na reduces the melting point and enhances the crystallization in 59S MBG and 59S 3DOM-BG.

***Acknowledgments***

This first author has received Ph.D. scholarship from Walailak University.

**REFERENCES**

1. A. Balamurugan, G. Sockalingum, J. Michel, J. Fauré, V. Banchet, L. Wortham, S. Bouthors, D. Laurent-Maquin and G. Balossier, Synthesis and characterisation of sol gel derived bioactive glass for biomedical applications, Materials Letters, 2006, **60** (29-30), 3752.
2. C. Wu and J. Chang, Mesoporous bioactive glasses: structure characteristics, drug/growth factor delivery and bone regeneration application-REVIEW, Interface Focus, 2012, **2** (3), 292.
3. Q. Z. Chen, Y. Li, L. Y. Jin, J. M.W. Quinn and P. A. Komesaroff, A new sol–gel process for producing $Na_2O$-containing bioactive glass ceramics, Acta Biomaterialia, 2010, **6** (10), 4143.
4. E. Dinu, M. Birsan, C. Ghiţulică, G. Voicu and E. Andronescu, Synthesis and characterization of hydoxyapatite obtained by sol–gel method, Romanian Journal of Materials, 2013, **43** (1), 55.
5. L. L. Hench, The story of Bioglass®, Journal of Materials Science: Materials in Medicine, 2006, **17** (11), 967.
6. T. Hyodo, K. Sasahara, Y. Shimizu and M. Egashira, Preparation of macroporous $SnO_2$ films using PMMA microspheres and their sensing properties to $NO_x$ and $H_2$, Sensors and Actuators B: Chemical, 2005, **106** (2), 580.
7. J. J. Blaker, J. E. Gough, V. Maquet, I. Notingher and A. R. Boccaccini, In vitro evaluation of novel bioactive composites based on Bioglass®-filled polylactide foams for bone tissue engineering scaffolds, Journal of Biomedical Materials Research, 2003, ***67A*** (4), 1401.
8. R. A. Martin, S. Yue, J. V. Hanna, P. D. Lee, R. J. Newport, M. E. Smith and J. R. Jones, Characterizing the hierarchical structures of bioactive sol−gel silicate glass and hybrid scaffolds for bone regeneration, Philosophical Transactions of the Royal Society A, 2012, **370** (1963), 1422.

9. D. Arcos and M. Vallet-Regí, Sol–gel silica-based biomaterials and bone tissue regeneration-REVIEW, Acta Biomaterialia, 2010, **6** (8), 2874.
10. D. Carta, D. M. Pickup, J. C. Knowles, M. E. Smith and R. J. Newport, Sol-gel synthesis of the $P_2O_5$-CaO-$Na_2O$-$SiO_2$ system as a novel bioresorbable glass, Journal of Materials Chemistry, 2005, **15** (21), 2134.
11. H. Yan, C. F. Blanford, W. H. Smyrlb and A. Stein, Preparation and structure of 3D ordered macroporous alloys by PMMA colloidal crystal templating, Chemistry Communications, 2000, **16**, 1477.
12. M. Klotz, A. Ayral, C. Guizard and L. Cot, Tailoring of the porosity in sol-gel derived silica thin layers, Bulletin of the Korean Chemical Society, 1999, **20** (8), 879.
13. C. J. Brinker, R. Sehgal, S. L. Hietala, R. Deshpande, D. M. Smith, D. Loy and C. S. Ashley, Sol-gel strategies for controlled porosity inorganic materials, Journal of Membrane Science, 1994, **94** (1), 85.
14. F. Branda, The sol-gel route to nanocomposites, Advances in Nanocomposites-Synthesis Characterization and Industrial Applications, InTech Publisher, 2011, 323.
15. J. R. Jones, Review of bioactive glass: From Hench to hybrids, Acta Biomaterialia, 2013, **9** (1), 4457.
16. C. J. Brinker, Hydrolysis and condensation of silicates: Effects on structure, Journal of Non-Crystalline Solids, 1988, **100** (1-3), 31.
17. G. E. Martin and S. H. Garofalini, Sol-gel polymerization: analysis of molecular mechanisms and the effect of hydrogen, Journal of Non-Crystalline Solids, 1994,**171** (1), 68.
18. P. Saravanapavan and L.L. Hench, Mesoporous calcium silicate glasses. I. Synthesis, Journal of Non-Crystalline Solids, 2003, **318** (1-2), 1.
19. J. R. Jones, S. Lin, S. Yue, P. D. Lee, J. V. Hanna, M. E. Smith and R. J. Newport, Bioactive glass scaffolds for bone regeneration and their hierarchical characterization, Proceedings of the Institution of Mechanical Engineers, Part H: Journal of Engineering in Medicine, 2010, **224** (12), 1373.
20. A. Lucas-Girot, F. Z. Mezahi, M. Mami, H. Oudadesse, A. Harabi and M. L. Floch, Sol– gel synthesis of a new composition of bioactive glass in the quaternary system $SiO_2$–CaO–$Na_2O$–$P_2O_5$ comparison with melting method, Journal of Non-Crystalline Solids, 2011, **357** (18), 3322.
21. J. Ma, C. Z. Chen, D. G. Wang and J. Z. Shi, Textural and structural studies of sol– gel derived $SiO_2$–CaO– $P_2O_5$–MgO glasses by substitution of MgO for CaO, Materials Science and Engineering C, 2010, **30** (6), 886.
22. M. I. El-Gohary, K. M. Tohamy, M. M. El-Okr, A. F. Ali and I. E. Soliman, Influence of composition on the in-vitro bioactivity of bioglass prepared by a quick alkali-mediated sol-gel method," Nature and Science, 2013, **11** (3), 26.
23. L. Leila, C. Jérôme, G. Laurent, Z. Rachid, T. Gilles, B. A. Didier and G. Alexandre, Structural transformations o bioactive glass 45S5 with thermal treatments, Acta Materialia, 2007, **55**(10), 3305.
24. I. Cacciotti, M. Lombardi, A. Bianco, A. Ravaglioli and L. Montanaro, Sol-gel derived 45S5 bioglass: synthesis, microstructural evolution and thermal behavior, Journal of Materials Science: Materials in Medicine, 2012, **23** (8), 1849.
25. L. Boroica, D. Radu, R. Medianu, I. C. Vasiliu and I. S. Boroica, Properties of glasses from $BaO$-$B_2O_3$-$TiO_2$ system, Romanian Journal of Materials, 2013, **43** (1), 68.

**********

## MANIFESTĂRI ŞTIINȚIFICE / SCIENTIFIC EVENTS

UNIVERSITATEA TEHNICĂ DIN CLUJ-NAPOCA
FACULTATEA DE CONSTRUCȚII

### C60 International Conference" Tradition and Innovation – 60 Years of Constructions in Transylvania" November 7, 2013 to November 9, 2013, Cluj-Napoca, Romania

The Conference aims at creating the opportunity of an exchange of experience, ideas and knowledge in the vast field of Construction industry. The summit of professionals, academics and the others involved in the Constriction activity may generate a comprehensive view on the overall performances, developments and tendencies in the fields of research, design and economics in the field.

The program will feature contributions (scientific papers, keynote lectures and posters) from scientists and practitioners on the following topics:

- Structural mechanics
- Soil mechanics and foundations
- Reinforced concrete structures
- Steel structures
- Buildings
- Roads, bridges and railways
- Construction technologies and management
- Building services
- Architecture and engineering graphics
- Challenges in teaching civil engineering

**Contact:** http://www.c60.ro
**E-mail:** dumitru.moldovan@dst.utcluj.ro

**********